Second International Conference on CFD in the Minerals and Process Industries
CSIRO, Melbourne, Australia
6-8 December 1999

A FINITE-VOLUME SHALLOW LAYER METHOD, FOR THE MHD INSTABILITIES IN AN ALUMINIUM PRODUCTION CELL

Laurent LEBOUCHER[1], Koulis PERICLEOUS[1], Ileana PANAITESCU[2] and Maurizio REPETTO[2]

[1] Centre for Numerical Modelling and Process Analysis, University of Greenwich,
30 Park Row, London SE10 9LS, UNITED KINGDOM
[2] Dipartimento di Ingeneria Elettrica Industriale, Politecnico di Torino,
Corso Duca degli Abruzzi 24, 10129 Torino, ITALY

ABSTRACT

An electrolytic cell for Aluminium production contains molten metal and molten electrolyte, which are subject to high dc-currents and magnetic fields. Lorentz forces arising from the cross product of current and magnetic field may amplify natural gravity waves at the interface between the two fluids, leading to short circuits in extreme cases. The external magnetic field and current distribution in the production cell is computed through a detailed finite element analysis at Torino Polytechnic. The results are then used to compute the magnetohydrodynamic and thermal effects in the aluminium/electrolyte bath. Each cell has lateral dimensions of 6m × 2m, whilst the bath depth is only 30 cm. The electrically resistive electrolyte path, which is critical in the operation of the cell, has a layer depth of only a few centimeters below each carbon anode. Because of the shallow dimensions of the liquid layer a finite-volume shallow-layer technique has been used at Greenwich to compute the resulting flow-field and interface perturbations. The information obtained from this method, i.e. depth averaged velocities and aluminium/electrolyte interface position is then embedded in the three-dimensional finite volume code PHYSICA and will be used to compute the heat transfer and phase change in the cell.

NOMENCLATURE

a	amplitude of the waves
$\mathbf{B}$	magnetic induction
c_0	phase velocity
g	acceleration due to gravity
h	depth of the layer
$\mathbf{j}$	perturbation to the current
$\mathbf{J}$	total electric current
l	wave length
l_x	short length of the bath
l_y	long length of the bath
N	interaction parameter
Re	Reynolds number
t	time
$\mathbf{u}$	velocity
$\mathbf{U}$	volume flux
U	x-component of the volume flux
V	y-component of the volume flux
x, y	horizontal coordinates
z	vertical coordinate

Greek Symbols

α	a/h_0
β	h_0^2/l_x^2
γ	l_x^2/l_y^2
δ	relative density difference
$\Delta\Phi$	potential drop through the electrolyte
η	displacement of the interface
κ	friction coefficient
Φ	electric potential
ρ	density
σ	electrical conductivity

Subscripts

0	single layer
1	upper layer
2	lower layer
t	partial time derivative
x, y	partial spatial derivatives
$\perp$	perpendicular to the interface
$\|\|$	parallel to the interface

SHALLOW WATER APPROXIMATION

Surface Waves

The depth-averaged Navier-Stokes equations are known as the shallow water equations. These equations give an approximation for the dynamics of long waves of length l and small amplitude a at the surface of a shallow layer of fluid of depth h_0. They express the conservation of mass and momentum and can be written in dimensional form in terms of the gravity g, the depth-averaged velocity $\mathbf{u}$ and displacement η of the surface height $h = h_0 + \eta$. Their dimensionless form is expressed in terms of the small parameters $\alpha = a/h_0$ and $\beta = h_0^2/l^2$;

$$\eta_t + \nabla \cdot [(1 + \alpha\eta)\mathbf{u}] = 0, \quad (1)$$

$$\mathbf{u}_t + \alpha\mathbf{u} \cdot \nabla\mathbf{u} + \nabla\eta - \frac{1}{3}\beta\nabla\nabla \cdot \mathbf{u}_t = O(\alpha^2, \alpha\beta), \quad (2)$$

the subscript t denoting partial time derivatives. The velocity $\mathbf{u}$ is scaled with ga/c_0, $c_0 = \sqrt{(gh_0)}$ being the linear phase velocity, the time t with l/c_0, the horizontal coordinate with l and the vertical displacement η with a. Neglecting the small terms in α and β gives a linear theory of waves which has been used by almost all authors in the field of interface instabilities in aluminium reduction cells, e.g. Sneyd[1]. The theories of nonlinear waves is reviewed in several books including Whitham[2] and Mei[3].

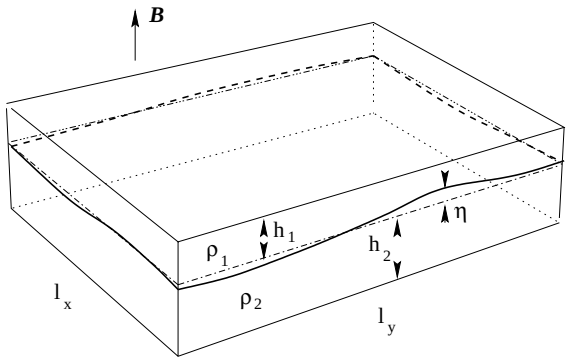

Figure 1: The two layers of fluid in an electrolytic bath and the perturbation $\eta(x,y)$ of the interface.

Two-layers Theory

Tomasson & Melville[4] have shown that the waves at the interface between two layers of fluids of similar densities can be represented by the same Boussinesq equations. Using the notations chosen by these authors, the top and bottom layers are respectively numbered 1 and 2 as shown on figure 1. Their densities are ρ_1, ρ_2 and their depths h_1, h_2. After introducing the equivalent single layer depth h_1, $h_0 = h_1h_2/(h_1+h_2)$ and the square of the linear phase speed $c_0^2 = gh_0\Delta\rho/\rho_0$, where $\Delta\rho = \rho_2 - \rho_1$ and $\rho_0 = (\rho_1+\rho_2)/2$ is a reference density, and assuming a balance between the volume fluxes $\mathbf{U}_1 = (h_1 - \eta)\,\mathbf{u}_1$ and $\mathbf{U}_2 = (h_2 + \eta)\,\mathbf{u}_2$ in the two layers, the single flux defined as $\mathbf{U}_1 = \mathbf{U}_2 = -\mathbf{U}_1$ satisfies the Boussinesq equations for the displacement η of the interface between the two fluids. Indeed, in dimensionless form and in terms of the small parameters $\alpha = a/h_0$ and $\beta = h_0^2/l_x^2$, scaling h_1 and h_2 with h_0, the densities ρ_2 and ρ_1 with ρ_0, the velocity flux $\mathbf{U}$ with h_2g_0a/c_0, the time t with l/c_0, the coordinates x and y with l and the vertical displacement η with a,

$$\eta_t + \nabla\cdot\mathbf{U} = 0, \tag{3}$$

$$\mathbf{U}_t + \alpha\left(\frac{1}{h_2}-\frac{1}{h_1}\right)[\mathbf{U}\cdot\nabla\mathbf{U} - (\eta\mathbf{U})_t] + \nabla\eta - \frac{1}{3}\beta h_1h_2\nabla\nabla\cdot\mathbf{U}_t = O(\alpha^2,\alpha\beta). \tag{4}$$

ALUMINIUM PRODUCTION CELL

An aluminium reduction cell is submitted to a strong electric current density **J** crossing both layers of fluid from the upper carbon anode to the lower carbon cathode. A significant magnetic field **B** mainly created by the input and output currents provided through "bus bars" to these two electrodes is also present. Any change in the position of the interface between the two liquid gives rise to a perturbation **j** in the current distribution as the electrical path in the electrolyte of poor conductivity σ_1 is either decreased or increased as shown on figure 2. Let us define $\Delta\Phi$ as the electric potential drop across the electrolyte. The vertical current density perpendicular to the interface is then defined in this fluid as

$$\mathbf{J}_\perp = -\sigma_1\nabla_\perp\Phi = \sigma_1\frac{\Delta\Phi}{h_1-\eta} \sim \sigma_1\frac{\Delta\Phi}{h_1}\left(1+\frac{\eta}{h_1}\right) = \mathbf{J}_{0\perp} + \mathbf{j}_\perp \tag{5}$$

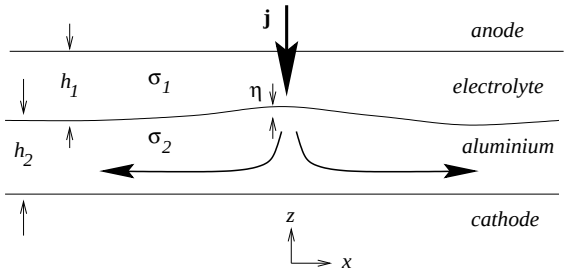

Figure 2: Perturbation of the electric currents due to the deformation of the interface between the molten aluminium and the electrolyte. The current takes the shortest path through the poorly conducting electrolyte.

The contribution of the interface perturbation in the normal current density $\mathbf{J}_\perp$ is therefore

$$\mathbf{j}_\perp = \frac{\sigma_1\Delta\Phi}{h_1^2}\eta \tag{6}$$

while the constant vertical current without deformation of the interface is just $\mathbf{J}_{0\perp} = \sigma_1\Delta\Phi/h_1$. The conservation law for electric charges may be written as

$$\nabla\cdot\mathbf{J} = \nabla\cdot\mathbf{j} = \nabla_\perp\cdot\mathbf{j}_\perp + \nabla_\parallel\cdot\mathbf{j}_\parallel = 0, \tag{7}$$

and may be integrated over the depth of the molten aluminium layer as

$$\begin{aligned}\int_{cathode}^{interface}\nabla\cdot\mathbf{j}\,\mathrm{d}z &= \nabla\cdot\int_{cathode}^{interface}\mathbf{j}_\parallel\,\mathrm{d}z + \int_{cathode}^{interface}\frac{\partial\mathbf{j}_\perp}{\partial z}\,\mathrm{d}z \\ &= \nabla_\parallel\cdot\langle\mathbf{j}_\parallel\rangle\times\int_{cathode}^{interface}\mathrm{d}z + [\mathbf{j}_\perp]_{cathode}^{interface} \\ &= (h_2+\eta)\,\nabla_\parallel\cdot\langle\mathbf{j}_\parallel\rangle + \mathbf{j}_\perp^{interface} = 0,\end{aligned} \tag{8}$$

where

$$\langle\mathbf{j}_\parallel\rangle = -\sigma_2\nabla_\parallel\Phi$$

is the depth-averaged current density in the molten aluminium and can be solved from the Poisson equation

$$\nabla_\parallel^2\Phi(x,y) = -\frac{\sigma_1}{\sigma_2}\frac{\Delta\Phi}{h_1^2h_2}\eta(x,y). \tag{9}$$

Since the electromagnetic force gives some energy and momentum to the fluid, the modelled interface oscillations can only increase if the dissipation due to the viscosity of the fluid is not taken into account. The linear friction law used by Bojarevics[5] is introduced in the model.

Scaling

Let us introduce the small parameter $\delta = (\rho_2-\rho_1)/(\rho_2+\rho_1)$ and the aspect ratio $\gamma = l_x^2/l_y^2$ of the bath horizontal dimensions so that the x- and y-coordinates are now scaled with l_x and l_y respectively. The time is scaled with l_x/c_0, the x- and y-components U and V of the velocity flux thus being scaled with αc_0h_0 and $\alpha\sqrt{\gamma}\,c_0h_0$. The linear friction law in $-\kappa\mathbf{U}$ used by Bojarevics[5] with a friction coefficient κ proportional to $\alpha\beta^{-1}\mathrm{Re}^{-1}$ is used. Defining the interaction parameter $N = (l_x^3\sigma_1\Delta\Phi B_{0\perp})/(l_yh_1^2\rho_2c_0^2)$ characterizing the ratio of electromagnetic to inertial forces and scaling the electric potential Φ with $(\sigma_1l_x^2a\Delta\Phi)/(\sigma_2h_1^2h_2)$ the dimensionless Boussinesq equations are

$$\eta_t + U_x + \gamma V_y = 0, \tag{10}$$

$$\left(1+\delta\frac{h_1-h_2}{h_1+h_2}\right)U_t+\alpha\left(\frac{1}{h_2}-\frac{1}{h_1}\right)\left[(UU)_x+\gamma(VU)_y-\eta U_t\right]$$
$$+\eta_x-\frac{1}{3}\beta h_1 h_2\left(U_{xxt}+\gamma V_{xyt}\right)=-N\Phi_y-\kappa U+O(\alpha^2,\alpha\beta,\alpha\delta,\beta\delta), \quad (11)$$

$$\gamma\left(1+\delta\frac{h_1-h_2}{h_1+h_2}\right)V_t+\alpha\gamma\left(\frac{1}{h_2}-\frac{1}{h_1}\right)\left[(UV)_x+\gamma(VV)_y-\eta V_t\right]$$
$$+\gamma\eta_y-\frac{1}{3}\beta\gamma h_1 h_2\left(U_{xyt}+\gamma V_{yyt}\right)=N\Phi_x-\gamma\kappa V+O(\alpha^2,\alpha\beta,\alpha\delta,\beta\delta), \quad (12)$$

the subscripts x and y denoting partial spatial derivatives.

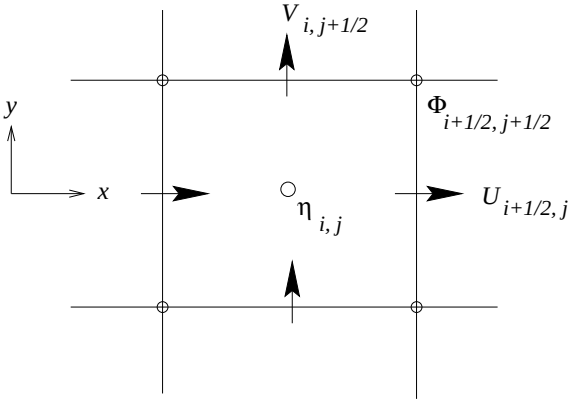

Figure 3: Finite volume mesh of the interface.

NUMERICAL METHOD AND SIMULATIONS

The finite volume method with a fully staggered grid as shown on figure 3 is used. All terms are computed with second order central finite differences for both spatial and time derivatives. The mass conservation equation (10) and the momentum equation (12) are solved alternatively. The perturbation η of the interface is computed explicitly at the time step n from its value at the time step n-1 and from the momentum (U,V) at the intermediate time step n-½:

$$\eta_{i,j}^{n}=\eta_{i,j}^{n-1}+\frac{\Delta t}{\Delta x}\left(U_{i+1/2,j}^{n-1/2}-U_{i-1/2,j}^{n-1/2}\right)$$
$$+\gamma\frac{\Delta t}{\Delta y}\left(V_{i,j+1/2}^{n-1/2}-V_{i,j-1/2}^{n-1/2}\right). \quad (13)$$

Then the electric potential can be solved from eq. (9) using a classical five-point finite difference scheme for the Laplacian of Φ and a four-point averaged value of $\eta_{I+½,j+½}$. The momentum U is computed implicitly at the time step n+½:

$$U_{i+1/2,j}^{n+1/2}=U_{i+1/2,j}^{n-1/2}+\Delta t\left[1+\left(\frac{1}{h_2}-\frac{1}{h_1}\right)\left(\delta-\alpha\eta_{i+1/2,j}^{n}\right)\right]^{-1}$$
$$\left\{-\alpha\left(\frac{1}{h_2}-\frac{1}{h_1}\right)\left[(UU)_x|_{i+1/2,j}^{n}+\gamma\,(VU)_y|_{i+1/2,j}^{n}\right]\right.$$
$$-\frac{\eta_{i+1,j}^{n}-\eta_{i,j}^{n}}{\Delta x}+\frac{1}{3}\beta h_1 h_2\left(U_{xxt}|_{i+1/2,j}^{n}+\gamma\,V_{xyt}|_{i+1/2,j}^{n}\right)$$
$$\left.-NB_{\perp i+1/2,j}^{n}\frac{\Phi_{i+1/2,j+1/2}^{n}-\Phi_{i+1/2,j-1/2}^{n}}{\Delta y}-\kappa U_{i+1/2,j}^{n}\right\} \quad (14)$$

where the x–component $(UU)_x + (VU)_y$ of the advection term is discretised in conservative form using a control volume centred at i+½, j and is averaged over the time steps n-½ and n+½, while the dispersion terms U_{xxt} and V_{xyt} are computed with second order central finite differences over two and three points for first and second order derivatives. The code is run with the parameters of the aluminium production plant in Slatina, Romania. The bath is 6 × 2 meters. The electrolyte and aluminium layers are 5 and 25 cm respectively. The imposed magnetic field is given by the commercial finite elements software CADEMA. The vertical component of the magnetic field is in the range to 10^{-3} to 10^{-2} T and the electric potential drop in the electrolyte is 1.5 V. The finite element mesh used to compute the main, i.e. *unperturbed*, electromagnetic field is shown on figure 4. The details of this FEM model can be found in reference[6].

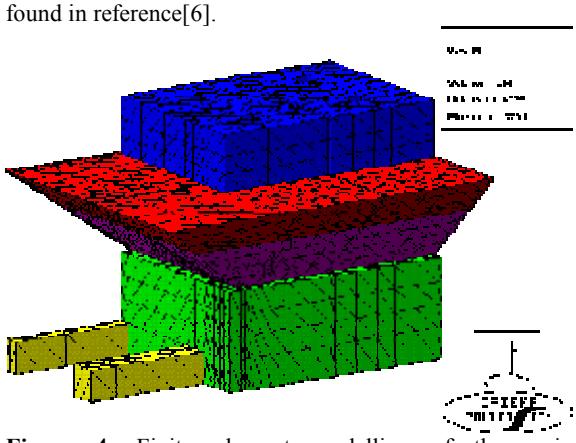

Figure 4: Finite element modelling of the main electromagnetic field.

Figure 5 gives an example of the simulation of a nonlinear wave after amplification of a linear perturbation by the Lorentz forces.

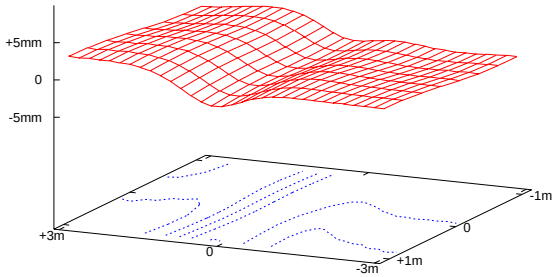

Figure 5: Example of the position $\eta(x,y)$ of the interface (vertical axis) between the molten aluminium and the electrolyte after amplification and nonlinear distortion of a small sine wave by the electromagnetic forces within the fluid.

The effect of the nonlinear α-terms and the dispersion β-terms appears to be essential. The interface takes a completely different shape from the initial sine wave. The amplitude of the waves loses its symmetry as shown on figures 6. Most important, this amplitude appears to be much less for the nonlinear waves than for the linear waves as shown by the one hour real time simulations (fig. 7) with and without the α- and β-terms.

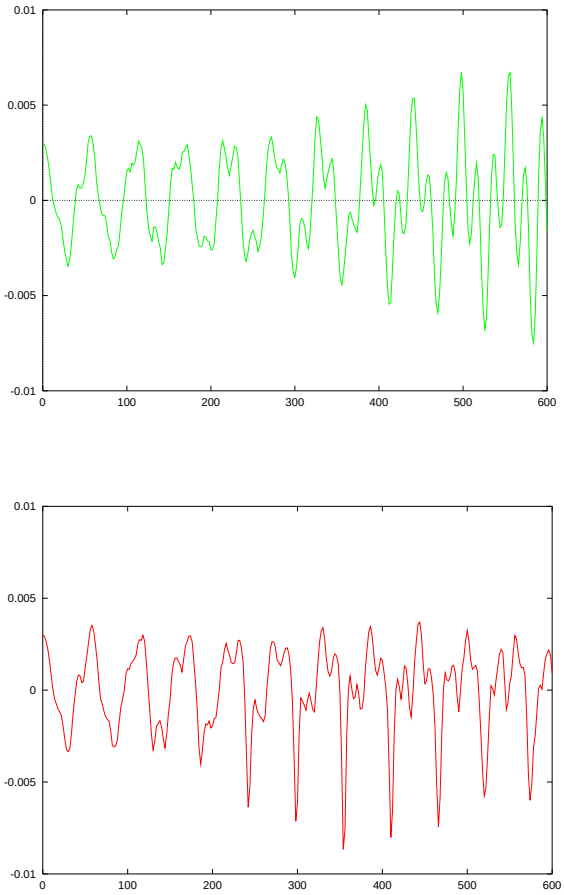

Figure 6: Evolution of the height η of the interface (y-axis, height in meters) at the corner of an aluminium reduction cell as a function of time (x-axis, time in seconds). Top: *linear* model. Bottom: *nonlinear* model with dispersion term.

CONCLUSION

The shallow layer equations discretised in finite volumes are successfully applied to model interface perturbations in an aluminium electrolysis cell. The effects of the nonlinear and the dispersion terms of the Boussinesq wave equations appear to be essential to the prediction of the amplification of aluminum interface instabilities. This finite volume formulation allows the integration of this model with standard computational fluid dynamics software for heat transfer computations, this work is in progress now.

ACKNOWLEDGMENTS

This work is funded by the European Union through the Copernicus contract IC 15-CT 96-0714.9

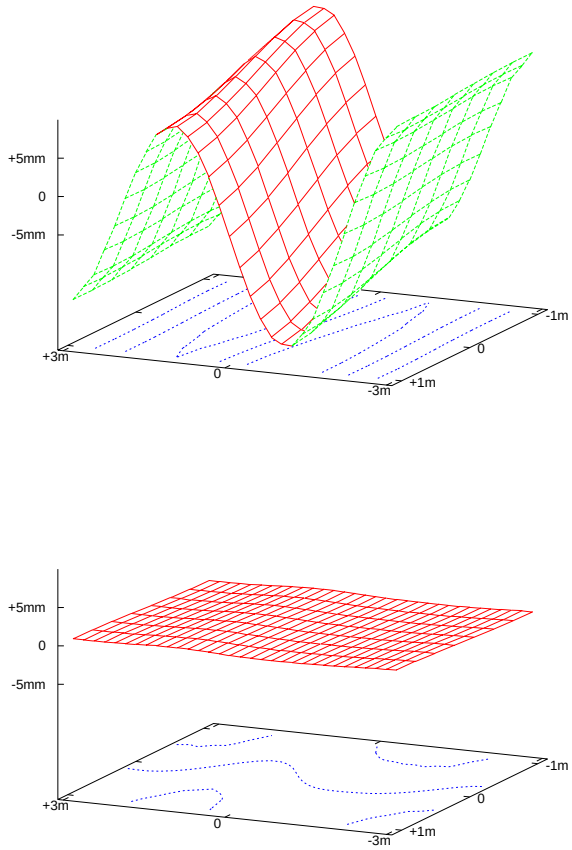

Figure 7: Interface position (vertical axis) after one hour of real time simulation. Top: linear model. Bottom: nonlinear model.

REFERENCES

1. SNEYD, A.D., WANG, A., "Interfacial instability due to MHD mode coupling in aluminium reduction cells", *J. Fluid Mech.*, **263**, pp. 343-359, 1994.
2. WHITHAM, G.B., *Linear and Nonlinear Waves*, John Whiley Sons, pp. 460-466, 1974.
3. MEI, C.C., *The Applied Dynamics of Ocean Surface Waves*, World Scientific, pp. 510, 1989.
4. TOMASSON, G.G. MELVILLE, W.K., "Geostrophic adjustment in a channel: nonlinear and dispersive effects", *J. Fluid Mech*., **241**, pp. 23-57, 1992.
5. BOJAREVICS, V., "Nonlinear waves with electro-gnetic interaction in aluminium electrolysis cells", Progress in Fluid Flow Research: Turbulence and Applied MHD, *AIAA* series on *Progress in Astronautics and Aeronautics*, **182**, pp. 833-848, 1998.
6. CHIAMPI, M., REPETTO, M., CHECHURIN, V., KALIMOV, A., LEBOUCHER, L., "Magnetic modelling and magnetohydrodynamic simulations of an aluminium production electrolytic cell", *COMPEL: the Int. J. for Computation and Mathematics in Electrical and Electronic Engning*, **18**, NO. 3, pp. 528-538, 1999.